ACS Macro Letters

Letter

pubs.acs.org/macroletters

Mixing of Two Immiscible Liquids within the Polymer Microgel Adsorbed at Their Interface

Rustam A. Gumerov,[†,‡] Artem M. Rumyantsev,[†,‡,§] Andrey A. Rudov,[‡,§] Andrij Pich,[§] Walter Richtering,[∥] Martin Möller,[§] and Igor I. Potemkin*[,‡,§]

[‡]Physics Department, Lomonosov Moscow State University, Moscow 119991, Russian Federation

[§]DWI – Leibniz Institute for Interactive Materials, Aachen 52056, Germany

[∥]Institute of Physical Chemistry, RWTH Aachen University, Aachen 52056, Germany

Supporting Information

ABSTRACT: We report on the behavior of two immiscible liquids within polymer microgel adsorbed at their interface. By means of dissipative particle dynamics (DPD) simulations and theoretical analysis in the framework of the Flory–Huggins (FH) lattice theory, we demonstrate that the microgel acts as a "compatibilizer" of these liquids: their miscibility within the microgel increases considerably. If the incompatibility of the liquids is moderate, although strong enough to induce phase separation in their 1:1 composition, they form homogeneous mixture in the microgel interior. The mixture of highly incompatible liquids undergoes separation into two (micro)-phases within the microgel likewise out of it; however, the segregation regime is weaker and the concentration profiles are characterized by a weaker decay (gradient) in comparison with those of two pure liquids. The enhanced miscibility is a result of the screening of unfavorable interactions between unlike liquid molecules by polymer subchains. We have shown that better miscibility of the liquids is achieved with densely cross-linked microgels. Our findings are very perspective for many applications where immiscible species have to be mixed at interfaces (like in heterogeneous catalysis).

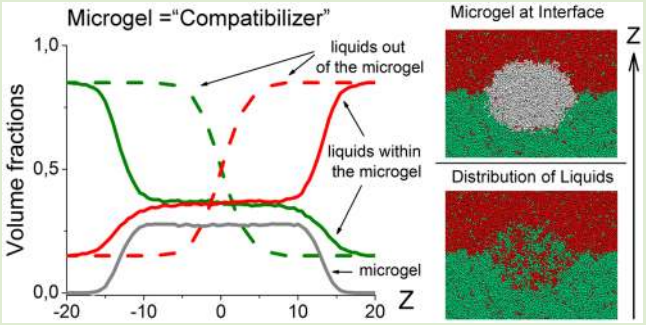

The ability of solid colloidal particles to efficiently stabilize emulsions has been known since the beginning of the 20th century.[1,2] In these systems, commonly called as Pickering emulsions, the degree of immersion of the colloidal particles into immiscible liquids as well as the contact angle are determined by the values of the surface tensions between particle, oil, and water. In turn, they govern surface curvature and volume of the stabilized droplets.[3] Once the particles are adsorbed at the interfaces, it is very difficult to control the values of the surface tensions by the external stimuli, and ultimately the size of the droplets and stability of the emulsions. Also, when densely packed at the interface, the particles strongly reduce the penetrability of the droplet surface by other dissolved substances hindering application of Pickering emulsions, for example, in catalysis.

In the middle of the past decade, it was proposed to use soft, adaptive polymer particles, that is, microgels instead of solid ones for the emulsion stabilization.[4−6] As compared to the rigid colloids, polymer microgels possess the ability to swell and the penetrability for low-molecular-weight substances. Being responsive to pH, temperature, and solution ionic strength, these particles can serve as a tool controlling droplet size and emulsion stability.[5−9] Alternation of external condition affecting microgel charge and degree of swelling may result in breaking of emulsions on demand, for example, in the case of P(NiPAM-*co*-MAA) microgels heating and pH reduction induce microgel shrinking that in turn makes the droplet interface more rigid, facilitating coalescence of oil droplets and resulting in emulsion breakage.[5,10] The sensitivity to external stimuli as well as microgel permeability makes the microgel-stabilized emulsions promising for many applications including biocatalysis.[11]

In this Letter we demonstrate one more effect, which makes the microgels even more attractive for emulsion stabilization. In addition to deformability,[12,13] increased coverage area and adsorption kinetics[14] in comparison with the solid counterparts, penetrability, and stimuli response, they can serve as compatibilizers of immiscible molecules. In particular, we demonstrate that two initially immiscible liquids, A and B (oil and water), can partially or fully be mixed within the microgel adsorbed at their interface. If the incompatibility of the liquids is relatively low, they form a homogeneous mixture within the whole microgel particle being segregated outside. As the incompatibility grows, separation into two (micro)phases within the microgel occurs. Enhanced liquid miscibility should

Received: February 20, 2016
Accepted: April 27, 2016
Published: May 2, 2016

DOI: 10.1021/acsmacrolett.6b00149
ACS Macro Lett. 2016, 5, 612−616

be attributed to the screening of unfavorable A−B contacts by the microgel subchains.

We performed dissipative particle dynamics[15−17] (DPD) simulations of a single spherical microgel particle placed at the interface of two immiscible liquids. Simulations were carried out in a cubic box of linear sizes $L_x = L_y = L_z = 60$ measured in units of the bead diameter. Details of the microgel design can be found in Supporting Information and refs 18 and 19. Total number of the beads in the microgel was chosen large enough, $M_{tot} = 12066$, to detect two distinct (micro)phases in the microgel interior, at least at high incompatibility of A and B liquids when the thickness of phase boundary was far fewer than the total microgel thickness in the direction perpendicular to the interface (z-axis). Each subchain comprises $M = 5$ beads.

The values of the interaction parameters between the beads of the liquids and polymer, a_{AP} and a_{BP}, were chosen in such a way to correspond to the cases when both liquids are good solvents for the microgel subchains and they interact with the microgel evenly, $a_{AP} = a_{BP} = 25$, and when one of the liquids (A) is a solvent of lower quality for the microgel than another (B), $a_{AP} = 26$ and 27, $a_{BP} = 25$. The DPD interaction parameters are related to the FH interaction parameters via[16] $\chi_{ij} = (0.286 \pm 0.002) \cdot (a_{ij} - 25)$. To provide liquid immiscibility, high enough values of $a_{AB} > 32$ (i.e., $\chi_{AB} > 2$) were chosen. The microgel tendency to occupy the AB interface should be attributed to the reduction of the surface tension due to the screening of unfavorable A−B contacts by polymer units. Similar effect is known for nanostructured block copolymers swollen in nonselective solvent which is inhomogeneously distributed in nanodomains with maxima at AB interfaces reducing surface tension.[20−25]

Snapshots of the system at $a_{AB} = 40$ ($\chi_{AB} = 4.29$) are shown in Figure 1. Good quality of a bottom solvent, $a_{BP} = 25$ ($\chi_{BP} = 0$), is also fixed. The first row (a) corresponds to the case when both liquids are equally good solvents, $a_{AP} = 25$ ($\chi_{AP} = 0$), and two other rows exhibit microgel structures in (b) a good upper solvent of slightly lower quality than the bottom one, $a_{AP} = 26$ ($\chi_{AP} = 0.286$), and in (c) an upper solvent being approximately Θ-solvent, $a_{AP} = 27$ ($\chi_{AP} = 0.572$). The left and the right images in each row correspond to visualization of one liquid only (B and A, respectively). Outside the microgel, a minor fraction of each liquid presents in the foreign liquid due to the entropic reasons: the higher the incompatibility of the liquids, the smaller the fraction in the foreign liquid. On the other hand, in the microgel location, distinct protrusion of both liquids is observed. The concentration of the corresponding liquid inside the microgel exceeds the average concentration of the minor fraction in the foreign liquid. It means that miscibility of two liquids within the microgel is higher than outside. Also, Figure 1 (middle snapshot in each row) demonstrates deformation (oblateness) of the microgel at the interface, which is promoted by minimization of AB interfacial energy and opposed by the elasticity of the subchains. This effect was detected in a number of experimental[12,26,27] and computer simulation[13,14] studies. The decrease of the solvent quality for one of the liquids (A) results in deeper immerse of the microgel into the better solvent (B),[27] Figure 1.

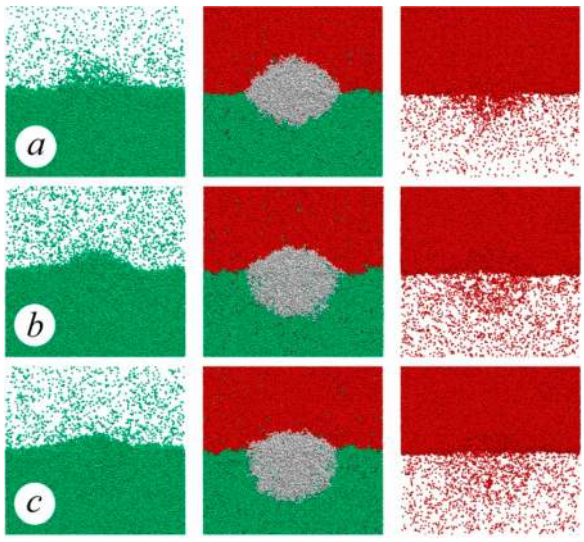

Figure 1. Snapshots of the microgel at the interface of two immiscible liquids at different combinations of the solvent quality of the liquids for the microgel. Left-to-right: distribution of B (green) molecules (the microgel and A molecules are not shown); side view of the microgel and two liquids; distribution of A (red) molecules. (a) Both liquids are equally good solvents for the microgel, $a_{AP} = a_{BP} = 25$. The decrease of the solvent quality of the red liquid, $a_{AP} = 26(b)$, $27(c)$, at fixed $a_{BP} = 25$ leads to deeper immersion of the microgel into the better solvent (green liquid); $a_{AB} = 40$.

For simplicity, hereafter we focus on the symmetric case assuming that A and B liquids interact with the microgel units identically. Dimensionless z-axis concentration profiles (volume fractions) of the two liquids (both are good solvents, $a_{AP} = a_{BP} = 25$) and the microgel are plotted in Figure 2 at different degrees of incompatibility of A and B liquids: $a_{AB} = 34$ ($\chi_{AB} = 2.57$), $a_{AB} = 45$ ($\chi_{AB} = 5.72$), and $a_{AB} = 60$ ($\chi_{AB} = 10.01$). These curves were obtained after averaging over the middle part of the microgel limited by one-third of its z-axis gyration radius, where its thickness is highest and hardly depends on the radial coordinate. Lateral (radial) density profiles can be found in Supporting Information, Figure S3. At moderate incompatibility (Figure 2a), the liquids are homogeneously mixed within the particle with equal volume fraction ($\phi_A = \phi_B$) owing to the symmetry of the system. If the liquids are strongly immiscible, two separate (micro)phases are observed within the microgel (Figure 2c). In this case, the density profiles have plateau inside the microgel (solid lines), which correspond to the concentration of the coexisting (micro)phases. Due to the presence of the microgel monomer units, the average concentration of the (micro)phases is smaller than outside (dashed lines) and the gradient of the concentration decay is smaller. Also, we can observe the increased concentration of monomer units at the interface (maximum of the polymer concentration at $z = 0$). This effect is due to the screening of unfavorable A−B interactions: polymer redistribution toward inner A−B interface, though accompanied by entropy penalty, diminishes the number of contacts between A and B molecules. It is similar to lamellae-forming diblock copolymers swollen in a nonselective solvent when concentration of low-molecular-weight solvent has maxima at nanodomain interfaces.[23] At intermediate values of A−B interaction parameters (Figure 2b), the thickness of the (micro)phase boundary is on the order of the microgel size and it is questionable to distinguish different (micro)phases. There is rather smooth gradient of concentration of the liquids in the microgels.

Increasing miscibility of the liquids inside the polymer microgel can be explained in the framework of the mean-field Flory−Huggins lattice theory.[28] We chose the lattice cell size equal to a, and all geometrical dimensions below are given in

DOI: 10.1021/acsmacrolett.6b00149
ACS Macro Lett. 2016, 5, 612−616

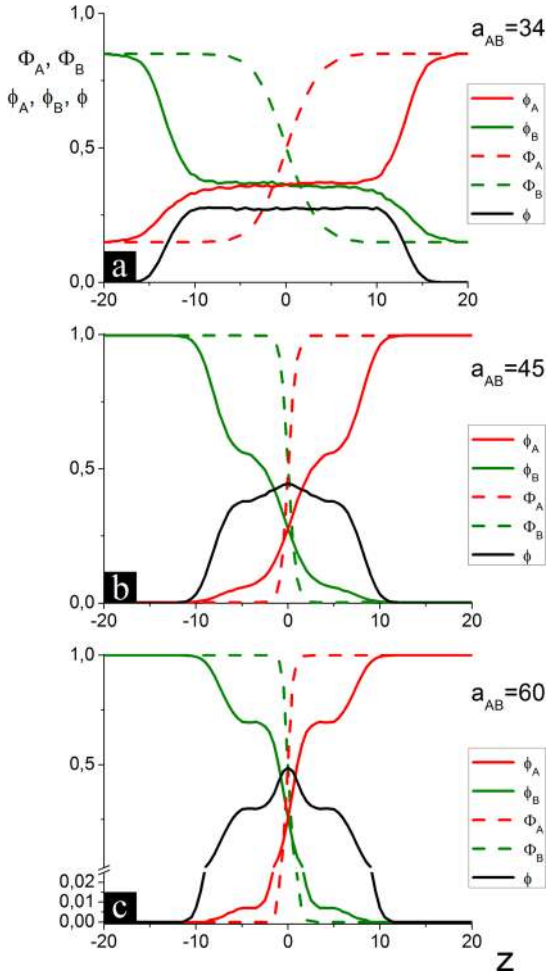

Figure 2. Concentrations of liquids A (red) and B (green) without microgel (dashed lines Φ_A and Φ_B) and within the microgel (solid lines ϕ_A, ϕ_B) as functions of normal coordinate z at different degrees of incompatibility of the liquids: (a) $a_{AB} = 34$; (b) $a_{AB} = 45$; (c) $a_{AB} = 60$. Black solid line ϕ depicts the polymer volume fraction; $a_{AP} = a_{BP} = 25$.

these units. Let ϕ_A, ϕ_B, and ϕ be volume fractions of the corresponding liquids and polymer within the microgel, and space-filling condition reads $\phi_A + \phi_B + \phi = 1$. Free energy density within the microgel (all energies here and below are in k_BT units) is given by

$$f_{in} = \varphi_A \ln \varphi_A + (1 - \varphi_A - \varphi) \ln(1 - \varphi_A - \varphi) + \chi_{AB}\varphi_A(1 - \varphi_A - \varphi) - \chi_{AP}(1 - \varphi)^2$$

where both liquids are considered to interact with the microgel equally, $\chi_{AP} = \chi_{BP}$, like in computer simulations. To analyze the range of stability of the homogeneous mixture of the liquids within the microgel, let us calculate the critical point $(\phi_A^{cr}; \chi^{cr})$ via solution of the equations $\partial^2 f_{in}/\partial\phi_A^2 = 0$ and $\partial^2 f_{in}/\partial\phi_A^3 = 0$:

$$\varphi_A^{cr} = \frac{1 - \varphi}{2}; \quad \chi^{cr} = \frac{2}{1 - \varphi} \tag{1}$$

In the case of pure liquids without the microgel, $\phi = 0$, eq 1 reproduces the well-known result $\phi_A^{cr} = 1/2$ and $\chi^{cr} = 2$. It is clearly seen that in the presence of the microgel, $\phi > 0$, miscibility of the liquids is enhanced: equal amounts of A and B liquids are subjected to phase separation without the microgel at $2 < \chi_{AB} < \chi^{cr}$ (above the spinodal of pure liquids), while they are homogeneously mixed inside the microgel within this χ_{AB}-range (below the spinodal). Densely cross-linked microgels providing higher values of ϕ promote the mixing of the liquids better as compared to loosely cross-linked ones. Note that the polymer volume fraction ϕ also depends on whether the liquids are mixed or exhibit phase separation that, in turn, affects microgel dimensions and volume. Moreover, the surface effects cannot be neglected. Thus, the above arguments are appealed to illustrate increasing liquid miscibility within the microgel, while more strict analysis is performed below.

Since microgel swelling (i.e., ϕ) depends on χ_{AB}, the total free energy of the microgel and the external solution should be constructed and minimized. We consider a microgel with ν subchains, each of N statistical segments of the length a, which undergoes anisotropic but uniform swelling (i.e., ϕ is assumed to be independent of spatial coordinates) being adsorbed at the flat interface between two immiscible liquids. The conformations of the subchains are quantified by two linear swelling coefficients: radial α_r and normal α_z. Elastic-free energy of the subchains can be written as[29]

$$F_{el} = \nu\left(\frac{1}{\alpha_r^2} + \frac{1}{2\alpha_z^2}\right) + \nu\left(\frac{\alpha_r^2}{3} - \frac{2N}{3}\ln\left(1 - \frac{\alpha_r^2}{N}\right) + \frac{\alpha_z^2}{6}\ln\left(1 - \frac{\alpha_z^2}{N}\right)\right)$$

where the subchains are assumed to have Gaussian dimensions in a reference state, so that the polymer volume fraction in this state $\phi_0 = \alpha_z\alpha_r^2\phi$. Free energy of interactions between A and B molecules and the microgel is given by

$$F_{vol} = V_{mg}(f_{in} - f_{out})$$

with microgel volume $V_{mg} = N\nu/\phi$ and

$$f_{out} = \Phi_A \ln \Phi_A + (1 - \Phi_A)\ln(1 - \Phi_A) + \chi_{AB}\Phi_A(1 - \Phi_A) - \chi_{AP}$$

with Φ_A being liquid A volume fraction in the outer solution. Finally, the excess free energy at the interface of these liquids, which is negligible in the case of macroscopic gel, should be also taken into account

$$F_{surf} = \pi\alpha_r^2 R_0^2(\gamma_{in} - \gamma_{out})$$

with the microgel radius in a reference state, $R_0 = (3N\nu/4\pi\phi_0)^{1/3}$, and dimensionless surface tensions given in k_BT/a^2 units

$$\gamma_{out} = 2\sqrt{\chi_{AB}} \int_{\Phi_{min}}^{\Phi_{maj}} d\Phi \sqrt{f_{out}(\Phi) - \mu_{out}\Phi + \Pi_{out}}$$

$$\gamma_{in} = 2\sqrt{\chi_{AB}} \int_{\varphi_{min}}^{\varphi_{maj}} d\varphi \sqrt{f_{in}(\varphi) - \mu_{in}\varphi + \Pi_{in}}$$

Coexisting phases are in chemical, $\mu_{in} = \mu_{out}$, and mechanical, $\Pi_{in} + d/d\phi(f_{in} + F_{el}/V_{mg})\phi - F_{el}/V_{mg} = \Pi_{out}$, equilibrium. Φ_{maj}, Φ_{min} are liquid A volume fractions in coexisting phases outside the microgel, and ϕ_{min}, ϕ_{maj} are the ones inside it. Minimization of the total free energy

$$F_{tot}(\alpha_r, \alpha_z) = F_{el} + F_{vol} + F_{surf}$$

with respect to the swelling coefficients α_r and α_z allows plotting binodals of the system (Figure 3). The values $N = 5$, $\nu = 2413$, $\varphi_0 = 0.5$, and $\chi_{AP} = 0$ (good solvent), corresponding to the microgel investigated in simulations, are fixed in subsequent calculations. The calculated binodals support the simple spinodal analysis. Two pure (without microgel) liquids coexist with each other above the binodal (dashed line in Figure 3). However, if parameters of the system correspond to the region

DOI: 10.1021/acsmacrolett.6b00149
ACS Macro Lett. 2016, 5, 612−616

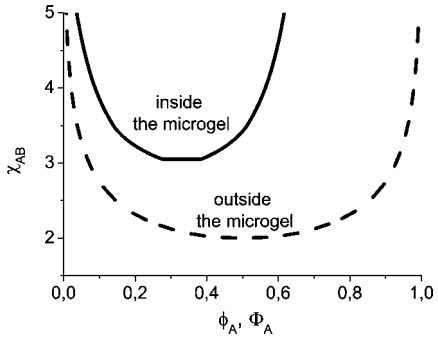

Figure 3. Binodals of two immiscible liquids outside the microgel (dashed) and inside the microgel (solid).

between the two binodals, two liquids are homogeneously mixed inside the microgel. Above the binodal of the microgel (solid line in Figure 3), the liquids are segregated in it.

To calculate the corresponding concentration profiles, we minimize the following functional[30]

$$\mathcal{F}\{\varphi_A(z)\} = \int_{-\infty}^{+\infty} (f_{in}(\varphi_A(z)) + k(\nabla\varphi_A(z))^2 + \mu_{in}\varphi_A(z))\mathrm{d}z$$

with $k = a^2\chi_{AB}$ and boundary conditions $\phi_A(-\infty) = \phi_{min}$, $\phi_A(+\infty) = \phi_{maj}$ at a fixed polymer volume fraction ϕ independent of z. The function $\Phi_A(z)$ was calculated in a similar way. Density profiles shown in Figure 4a, c, and d correspond to those in Figure 2a–c since respective values of the FH interaction parameter χ_{AB} and the DPD simulation parameter a_{AB} match, $\chi_{AB} = 0.286 \cdot (a_{AB} - 25)$. Detailed comparison of the theoretical and simulation results is shown in Supporting Information, Figures S4 and S5.

At relatively low values of χ_{AB} (Figure 4a) the liquids form homogeneous mixture within the particle, $\phi_A = \phi_B = \mathrm{const}(z)$. As FH interaction parameter exceeds critical value $\chi_{AB}^{cr} = 3.01$, the liquids segregate symmetrically within the microgel. However, the volume fractions of the liquids in foreign phases are bigger in comparison with those outside the microgel (Figure 4b–d). It is also seen that phase boundary inside the microgel is thicker than outside. In a strong segregation limit, $\chi_{AB} \gg 1$, the volume fraction of the liquid in the foreign phase is given by $\Phi_{min} \approx e^{-\chi_{AB}}$ in the outer solution and $\phi_{min} \approx e^{-(1-\phi)\chi_{AB}}$ within the microgel. If the liquids are highly incompatible (e.g., $\chi_{AB} = 10$), the values ϕ_{min} and Φ_{min} may differ 10 times, even in a rather loosely cross-linked microgel ($\phi = 0.23$). The value of the surface tension inside the microgel in this limit is given by $\gamma_{in} \approx \pi\chi_{AB}(1-\phi)^2/4$, that is $1/(1-\phi)^2$ times lower than the surface tension between A and B liquids outside the microgel. The effect of oil–water surface tension diminution as a consequence of microgel adsorption to the interface has been experimentally observed, and temperature-sensitive microgels reduce surface tension in a collapsed state (i.e., above VPTT) stronger than in a swollen one (i.e., below VPTT),[31] in accordance with the theoretical prediction described above.

The miscibility of liquids is governed by the interplay between the gain in translational entropy and the loss in the interaction energy between A and B molecules. Since the symmetric case is considered, entropy gain under mixing of equal volumes of A and B liquids equals to k_B ln 2, regardless of mixing that happens within or without the microgel. However, the energy penalty because of unfavorable A–B interactions is proportional to the probability that an A molecule has a contact

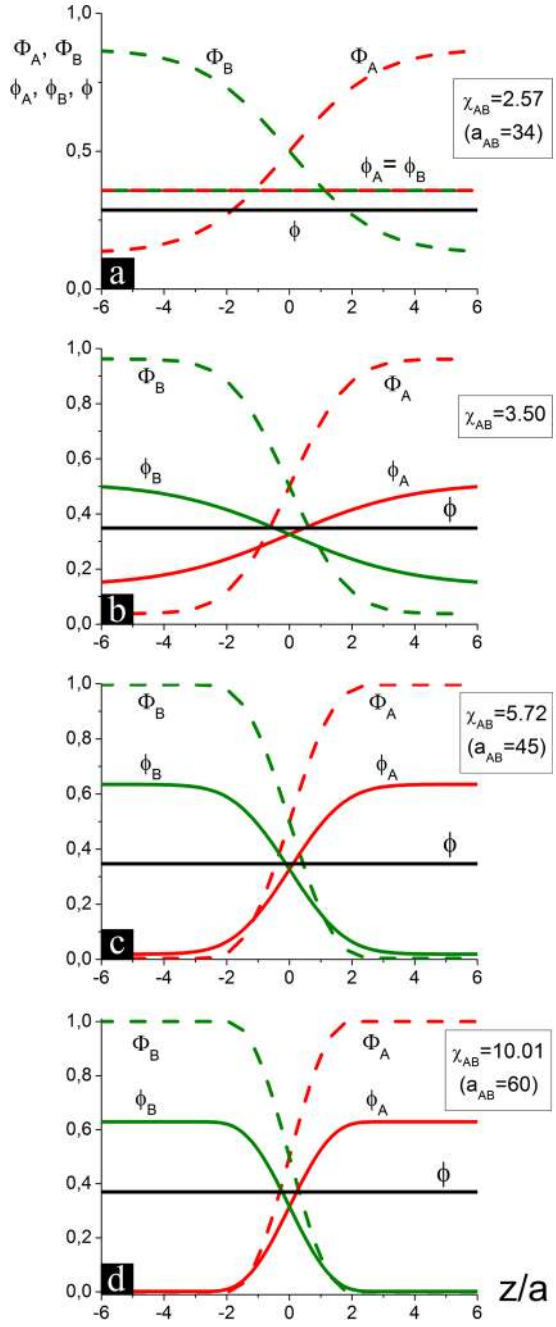

Figure 4. Concentrations of liquids A (red) and B (green) outside microgel (dashed lines Φ_A and Φ_B), inside the microgel (solid lines ϕ_A, ϕ_B), and polymer volume fraction (ϕ) as functions of normal coordinate z at different values of the FH interaction parameter between A and B liquids.

with the molecule B, that is, to $\phi_B = (1-\phi)/2$. Thus, the microgel subchains screen unfavorable A–B interactions, and the microgel serves as efficient compatibilizer of immiscible liquids.

To conclude, the ability of polymer microgels to enhance miscibility of liquids was revealed by means of DPD simulations and explained theoretically in terms of the FH lattice model. Moderately immiscible liquids can form a thermodynamically stable homogeneous mixture within the microgel. In the case of strong incompatibility of the liquids, phase separation into two (micro)phases enriched by different components occurs. However, these (micro)phases are characterized by lower

DOI: 10.1021/acsmacrolett.6b00149
ACS Macro Lett. 2016, 5, 612–616

difference in concentrations and wider interfacial thickness in comparison with the coexisting phases outside the microgel. The physical reason for the enhanced compatibility of the liquids inside the microgel is related to the screening of unfavorable A−B contacts by monomer units of the microgel. One of the experimental systems, where the predicted effect could be observed, is poly(*N*-vinylcaprolactam) (PVCL) microgel adsorbed at water−toluene interface. Water and toluene can be considered as immiscible solvents (solubility of toluene in water is very low: 0.52 g/L at 20 °C[32]). However, both solvents are good solvents for PVCL chains.[33] The discovered effect opens new possibilities for optimization of extraction/separation processes and design of new catalyst systems for efficient and sustainable chemical transformations.

■ ASSOCIATED CONTENT

Supporting Information

The Supporting Information is available free of charge on the ACS Publications website at DOI: 10.1021/acsmacrolett.6b00149.

Details on computer simulations and Figures S1−S5 (PDF).

■ AUTHOR INFORMATION

Corresponding Author

*E-mail: igor@polly.phys.msu.ru.

Author Contributions

†These authors contributed equally to this work (R.A.G. and A.M.R.).

Notes

The authors declare no competing financial interest.

■ ACKNOWLEDGMENTS

The financial support of the Russian Foundation for Basic Research (projects 15-33-21151 and 16-03-00266), the Deutsche Forschungsgemeinschaft within SFB 985 and the Volkswagen Foundation is gratefully acknowledged. The simulations were performed on multiteraflop supercomputer Lomonosov at Moscow State University.

■ ABBREVIATIONS

VPTT volume phase transition temperature; P(NiPAM-*co*-MAA) poly(*N*-isopropylacrylamide-*co*-methacrylic acid)

■ REFERENCES

(1) Ramsden, W. *Proc. R. Soc. London* **1903**, *72*, 156−164.
(2) Pickering, S. U. *J. Chem. Soc., Trans.* **1907**, *91*, 2001−2021.
(3) Nallamilli, T.; Mani, E.; Basavaraj, M. J. *Langmuir* **2014**, *30*, 9336−9345.
(4) Amalvy, J. I.; Armes, S. P.; Binks, B. P.; Rodrigues, J. A.; Unali, G.-F. *Chem. Commun.* **2003**, *14*, 1826−1827.
(5) Ngai, T.; Behrens, S. H.; Auweter, H. *Chem. Commun.* **2005**, *17*, 1014−1018.
(6) Fujii, S.; Read, E. S.; Binks, B. P.; Armes, S. P. *Adv. Mater.* **2005**, *17*, 1014−1018.
(7) Ngai, T.; Auweter, H.; Behrens, S. H. *Macromolecules* **2006**, *39*, 8171−8177.
(8) Richtering, W. *Langmuir* **2012**, *28*, 17218−17229.
(9) Li, Z.; Ngai, T. *Nanoscale* **2013**, *5*, 1399−1410.
(10) Brugger, B.; Rosen, B. A.; Richtering, W. *Langmuir* **2008**, *24*, 12202−12208.
(11) Wiese, S.; Spiess, A. C.; Richtering, W. *Angew. Chem., Int. Ed.* **2013**, *52*, 576−579.
(12) Geisel, K.; Isa, L.; Richtering, W. *Langmuir* **2012**, *28*, 15770−15776.
(13) Geisel, K.; Rudov, A. A.; Potemkin, I. I.; Richtering, W. *Langmuir* **2015**, *31*, 13145−13154.
(14) Mourran, A.; Wu, Y.; Gumerov, R. A.; Rudov, A. A.; Potemkin, I. I.; Pich, A.; Möller, M. *Langmuir* **2016**, *32*, 723−730.
(15) Hoogerbrugge, P. J.; Koelman, J. M. V. A. *Europhys. Lett.* **1993**, *21*, 363−368.
(16) Groot, D.; Warren, P. B. *J. Chem. Phys.* **1997**, *107*, 4423−4435.
(17) Maiti, A.; McGrother, S. *J. Chem. Phys.* **2004**, *120*, 1594−1601.
(18) Rumyantsev, A. M.; Rudov, A. A.; Potemkin, I. I. *J. Chem. Phys.* **2015**, *142*, 171105.
(19) Schroeder, R.; Rudov, A. A.; Lyon, L. A.; Richtering, W.; Pich, A.; Potemkin, I. I. *Macromolecules* **2015**, *48*, 5914−5927.
(20) Rudov, A. A.; Khalatur, P. G.; Potemkin, I. I. *Macromolecules* **2012**, *45*, 4870−4875.
(21) Fredrickson, G. H.; Leibler, L. *Macromolecules* **1989**, *22*, 1238−1250.
(22) Lodge, T. P.; Hamersky, M. W.; Hanley, K. J.; Huang, C.-I. *Macromolecules* **1997**, *30*, 6139−6149.
(23) Rudov, A. A.; Patyukova, E. S.; Neratova, I. V.; Khalatur, P. G.; Posselt, D.; Papadakis, C. M.; Potemkin, I. I. *Macromolecules* **2013**, *46*, 5786−5795.
(24) Glagoleva, A.; Erukhimovich, I.; Vasilevskaya, V. *Macromol. Theory Simul.* **2013**, *22*, 31−35.
(25) Stenbock-Fermor, A.; Rudov, A. A.; Gumerov, R. A.; Tsarkova, L. A.; Böker, A.; Möller, M.; Potemkin, I. I. *ACS Macro Lett.* **2014**, *3*, 803−807.
(26) Destribats, M.; Lapeyre, V.; Wolfs, M.; Sellier, E.; Leal-Calderon, F.; Ravaine, V.; Schmitt, V. *Soft Matter* **2011**, *7*, 7689−7698.
(27) Schmidt, S.; Liu, T.; Rutten, S.; Phan, K.-H.; Möller, M.; Richtering, W. *Langmuir* **2011**, *27*, 9801−9806.
(28) Flory, P. J. *Principles of Polymer Chemistry*; Cornell University Press: New York, 1953.
(29) Jha, P. K.; Solis, F. J.; de Pablo, J. J.; de la Cruz, M. O. *Macromolecules* **2009**, *42*, 6284−6289.
(30) Cahn, J. W.; Hilliard, J. E. *J. Chem. Phys.* **1958**, *28*, 258−267.
(31) Wu, Y.; Wiese, S.; Balaceanu, A.; Richtering, W.; Pich, A. *Langmuir* **2014**, *30*, 7660−7669.
(32) Neely, B. J.; Wagner, J.; Robinson, R. L.; Gasen, K. A. M. *J. Chem. Eng. Data* **2008**, *53*, 165−174.
(33) Kirsch, Y. E. *Prog. Polym. Sci.* **1993**, *18*, 519.

DOI: 10.1021/acsmacrolett.6b00149
ACS Macro Lett. 2016, 5, 612−616